The Pierre Auger Observatory and its Fluorescence Detector

S. Argirò [a] for the Auger Collaboration

[a] Università degli Studi di Torino and INFN

The Pierre Auger Cosmic Ray Observatory is designed to elucidate the origin and nature of Ultra High Energy Cosmic Rays (UHECR). With an unprecedented aperture and sensitivity, and with the use of a hybrid technique, it will be able to collect and characterize a large number of Extensive Air Showers generated by primaries with energies greater than 10^{19} eV. In this paper we describe the Fluorescence Detector and its operation during the first phase of the experiment, called *Engineering Array*.

1. Introduction

Experimental evidence of air showers generated by primaries above 10^{20} eV is reported by various experiments using different techniques [1], [2]. This evidence raises several questions. First, it is not clear what kind of mechanism is able to accelerate the primaries to such energy. Furthermore, the problem of propagation exists: simple considerations, in fact, predict that a proton of $E > 10^{20}$ eV cannot propagate for more than 100 Mpc, due to interaction with the Cosmic Microwave Background (the GZK cutoff [3], [4]). Finally, the problem of the arrival direction and its isotropy or anisotropy deals with the distribution of sources and the pattern of intergalactic magnetic fields.
The experimental situation is at the moment unclear, with some experiments claiming detection of anisotropy and observation of GZK - violating features of the flux [1], some experiments claiming the opposite [5]. Only a dramatic increase of the statistics and a robust experimental technique can disentangle the problem.

2. The need for a hybrid detector

Most UHECR experiments use either the ground array technique, in which the secondary particles are detected at ground level, or the air fluorescence technique, in which the shower longitudinal profile is tracked. The use of both techniques in combination could help understanding the incompatibilities, and would offer an instrument of unprecedented precision. The fluorescence detector has a duty cycle of 10-15% (in fact it runs on clear nights when the moon is below 50%). The corresponding fraction of events can be used to calibrate the Surface Detector, which determines the energy in a way that has some dependence on the hadronic interaction modeling.

The hybrid reconstruction method improves upon what can be achieved by either the FD or the SD on its own [6]. Core locations have been determined using the engineering hybrid data with an uncertainty of approximately 100 meters. Arrival directions in the engineering data are determined to a fraction of a degree. The geometric uncertainties are already small enough to have little effect on the determination of shower energy and depth of maximum, and are expected to improve with an upgrade of the timing hardware. Calibration uncertainties are also small. Statistical uncertainties will be appropriately dominated by Poisson limitations in the collected signal and background, except at very high energies where the signal-to-noise will be especially large. New measurements of the atmospheric fluorescence yield and new methods of atmospheric aerosol monitoring are being pursued to reduce the systematic errors that may dominate the uncertainties in energy and depth of maximum.

3. The Pierre Auger Observatory

The Pierre Auger Observatory will consist of two sites, one in the northern, one in the southern hemisphere, each supporting a detection area of about 3000 km^2. This has to be compared with an expected flux of about 1/year/km^2/sr above 10^{19} eV and 0.01 /year/km^2/sr above 10^{20} eV. The instrument will use a hybrid technique. At each site, 1600 water Cerenkov detectors, placed in a hexagonal grid with

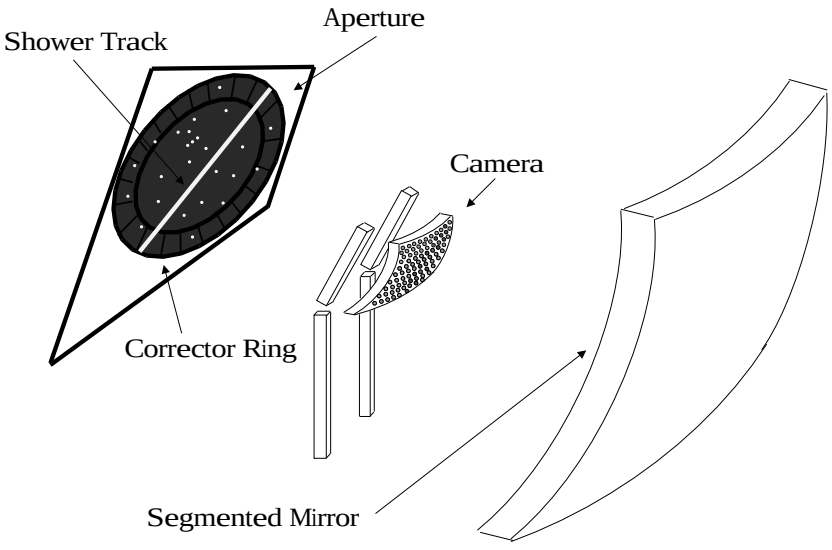

Figure 1. Schematic view of the Fluorescence Telescope

1500 m spacing, will be overlooked by 24 air fluorescence telescopes. While the ground array detects secondary particles, giving a direct measurement of the lateral distribution function, the fluorescence detector records fluorescence photons as a function of time, therefore measuring the longitudinal development of the shower.
An engineering hybrid prototype consisting of 32 ground detectors and two fluorescence telescopes (corresponding to a field of observation of 60° in azimuth and 30° in elevation) has been successfully operated from December 2001 to March 2002.

4. The Surface Detector

Each ground station consists of a cylindrical water tank with $10m^2$ top area and 1.2m height. Three PMTs detect Cerenkov light produced by muons and electrons traversing the radiator. The station is powered by means of solar panels and batteries, and communicates with the Central Data Acquisition via a wireless link. The signal of each PMT is sampled at 40 MHz by two 12 bit FADC, one reading out the anode and one the last dynode. Two levels of local trigger are implemented at the station, while the third level trigger fires when four stations are hit, achieving full efficiency above 10^{19} eV. The goal of the ground detector is the determination of the particle density at 1000 m from the core [6], which is related to primary energy, while the shower geometry can be inferred from the arrival time of the shower front at different tanks. In addition, the time structure of the signal is measured, which makes the detector sensitive to primary composition.

5. The Fluorescence Detector

In the following sub-sections the Fluorescence Detector of the Auger Observatory will be described.

5.1. Fluorescence Physics

When the electrons of the shower interact with the nitrogen in the atmosphere, fluorescence photons are

emitted isotropically, with wavelengths in the range 300-420 nm. Each electron emits four to five photons per meter of track length, depending on the temperature and pressure and therefore on altitude [7]. From the number of photons, one can infer the shower size at each atmospheric depth (X). The light signal originating in a layer between X and $X + \delta X$ (where δX depends on the sampling) and received by the detector is given by:

$$S(X) = F_y(h) n_e(X) \frac{A}{4\pi r^2}\, c\, \delta t \cdot \epsilon \cdot \mathcal{T}(r) \quad (1)$$

where $F_y(h)$ is the fluorescence yield at the emission altitude h, A is the collection area, r the observation distance, δt is the time the shower takes to travel from X to $X + \delta X$ when viewed from the detector (δt depends solely on the geometry), ϵ is the collection efficiency and $\mathcal{T}(r)$ factorizes the transmission of the atmosphere. The atmosphere in the sensitive volume of the Observatory is characterized by means of Lidars, Horizontal Attenuation Monitors, weather stations, cloud monitors and radiosondes.
The contribution of direct and scattered Cerenkov light must be subtracted. The electromagnetic energy can then be calculated as:

$$E_{em} = \frac{E_c}{X_r} \int n_e(X) dX \quad (2)$$

where $n_e(X)$ is the number of electrons at depth X[$\frac{g}{cm^2}$], E_c is the critical energy of electrons in air and X_r their radiation length.

5.2. Optics

The Auger collaboration has selected a Schmidt optics for the fluorescence telescopes, which structure is shown in figure 1. A telescope unit consists of a spherical mirror, composed of 36 to 60 subsegments, with a radius of curvature of 3400 mm. On the focal surface is a camera of 440 photomultipliers (pixels), each with 1.5 $\times$ 1.5 deg^2 field of view. The camera surface is also quasi-spherical, with R$\simeq$1700mm . To fill the gaps between the hexagonal photomultipliers, special light collection devices have been engineered [8]. The circular aperture has a diameter of 2.20 m and features both an optical filter (MUG-6) to select fluorescence photons in the range 300-400 nm [9] and the *Corrector Ring*. This is an annular Schmidt lens 25 cm wide, effectively doubling the collection area without degrading the image with spherical or coma aberration. This feature is particularly important when taking into account that the signal to noise ratio is proportional to the aperture radius.
The above geometry results in a field of view of 30° in elevation and 30° in azimuth for each telescope unit. Groups of six telescopes form an *eye* with 180° view in azimuth. Four such eyes overlook the 3000 km^2 ground array.

5.3. Electronics

The readout of each PMT is of the *current sampling* type. The waveform is sampled at 10 MHz with a 12 bit resolution and 15 bit dynamic range, as described below. The structural diagram of the electronic chain is shown in figure 2 Attached to the PMT is the *Head Electronics*, which consists of a *bias printed circuit board (pcb)* and a *driver pcb*. The bias to the PMT is designed to achieve low power and high linearity even in presence of a large DC current, such as the current induced by the night sky background, which is of the order of 0.5 μA for dark sky, but increases to 3.7 μA when a star is in the field of view, or to 2 μA in presence of scattered moonlight. The *driver pcb* implements a differential line driver with a high rejection of common mode noise. The signals out of the drivers are collected at the *Distribution Boards* and routed to the *Front End Crate* .
Each crate serves one telescope, and contains twenty *First Level Trigger (FLT) / Analog Boards* and one *Second Level Trigger (SLT)* board. Each FLT / Analog Board serves 22 channels, or a column of pixels in the camera. The *Analog Board* processes the signal prior to sampling. It implements a receiver section, an anti aliasing Bessel filter and a programmable gain section. The 15 bit dynamic range with a 12 bit FADC is achieved through the following technique. Each pixel is processed with the normal *high gain* channel. The sum of eleven pixels (even or odd in a column) is processed by a virtual *low gain* channel. If one pixel in the group of eleven saturates, the signal can be obtained from the virtual channel. Thanks to the pixel arrangement and the time characteristics of the fluorescence signal, at most one channel saturates in the group [10].
The FLT board samples the analog signal of each channel at 10 MHz and provides the first level trigger, or pixel trigger. A boxcar running sum of ten FADC

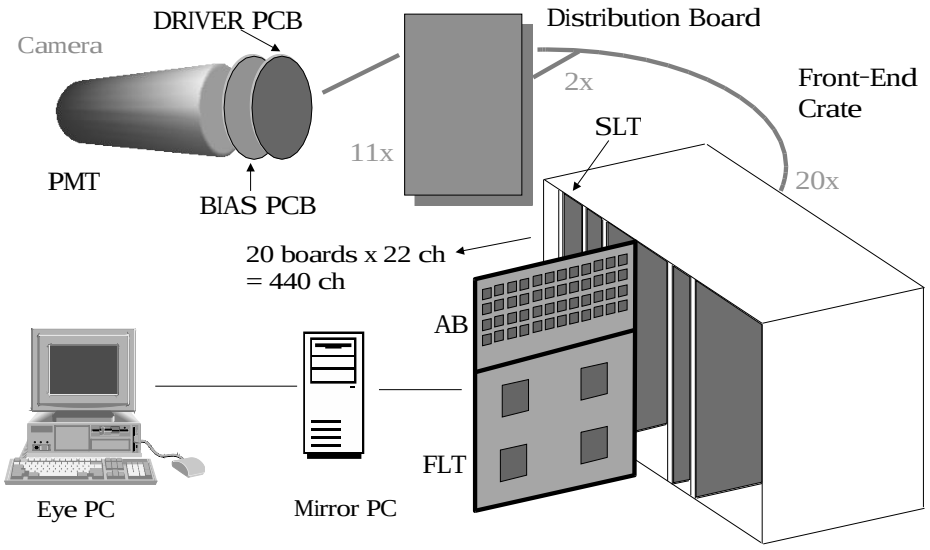

Figure 2. Schematic view of the DAQ chain of a Fluorescence telescope

samples is performed and compared with a threshold value. This threshold changes dynamically to keep the trigger rate close to 100 Hz. Fired pixels are then scanned by the second level trigger (SLT), or camera trigger, which recognizes patterns induced by a fluorescence track. The FLT flag for a single pixel persists 20μs, and the camera is scanned for patterns every other μs. The SLT rate during the EA run was around 0.3 Hz.

Each *Front End Crate* is connected to a *Mirror PC*, which runs the processes that take care of its acquisition. On the *Mirror PC* runs the *Third Level Trigger*. This is a software trigger that is responsible for rejection of background events. These events consist mainly of muons hitting directly the camera and lightnings. The 3^{rd} level trigger rate was around 8×10^{-4} Hz.

The six *Mirror PC's* are then connected to the *Eye PC*, on which event building and run control take place.

5.4. Detector Calibration

Absolute detector calibration is required for the air fluorescence measurement. The strategy envisaged for the Auger Fluorescence Detector is the following. Each telescope undergoes an absolute calibration monthly, with the method of the *drum calibration*. Between absolute calibrations, that is for every night of observation or even several times within the night, a relative calibration is performed using a set of optical fibers which carry the light from a xenon lamp.

The *drum* calibration device consists of two layers of diffusely reflective material, holding in the center a calibrated light source. The outer drum surface is translucent to allow photon emission. It reflects and diffuses light in every direction, with anisotropies less than 2% in the region of interest. The light output is measured by means of calibrated PMTs. The *drum* is placed at the aperture and therefore illuminates all pixel directions uniformly. Knowing the light flux and comparing with the detector response, absolute calibration is achieved.

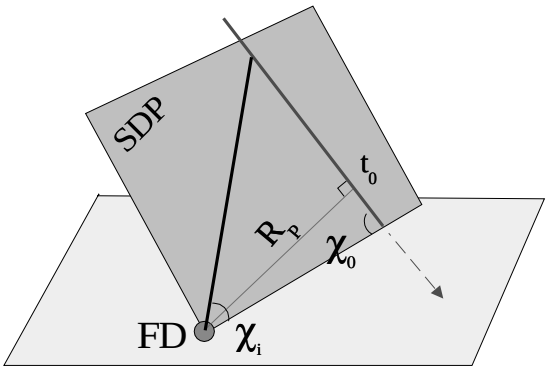

Figure 3. The geometry of the air shower axis with respect to the fluorescence detector

5.5. Reconstruction techniques

The first step in reconstructing a shower with the Fluorescence Detector is finding the Shower Detector Plane (SDP), which is the plane defined by the detector and the shower axis. This is done selecting the trial plane that minimizes the distance from the hit pixels directions. In second place one must find the position of the shower axis within the SDP. This can be done in three ways. If the event is seen in monocular mode, the *time fit* can be used. The geometrical parameters that describe the shower in the SDP are R_P (distance shower-detector), t_0 (time when the point of minimum distance is reached) and χ_0 (angle between shower and ground) (see fig. 3). These parameters are related to the hit times (time when the light reaches the pixel) by:

$$t(\chi_i) = t_0 + \frac{R_p}{c} tan \frac{(\chi_0 - \chi_i)^2}{2} \qquad (3)$$

and can be found by minimization of the quantity $\chi^2 = \sum \frac{(t_i - t_{\chi_i})^2}{\sigma_{t_i}}$, where t_i is the measured hit time for the i^{th} pixel. If the event was detected in hybrid mode, the point and time of impact of the shower with the ground adds a useful constraint to the fit. Finally, if the shower was detected by two *eyes*, the two SDPs can be intersected to find the shower axis.

Once the shower geometry is determined, the light profile at diaphragm, or the number of photons impinging on the aperture versus time, is found. At this point, eq. 1 can be used to estimate the number of particles at each atmospheric depth. The contribution of direct and scattered Cerenkov light must be subtracted. The resulting profile can then be fit using a Gaisser-Hillas parametrization, eq. 2 being used to estimate the primary energy. Figure 4 shows an example of a reconstructed shower profile.

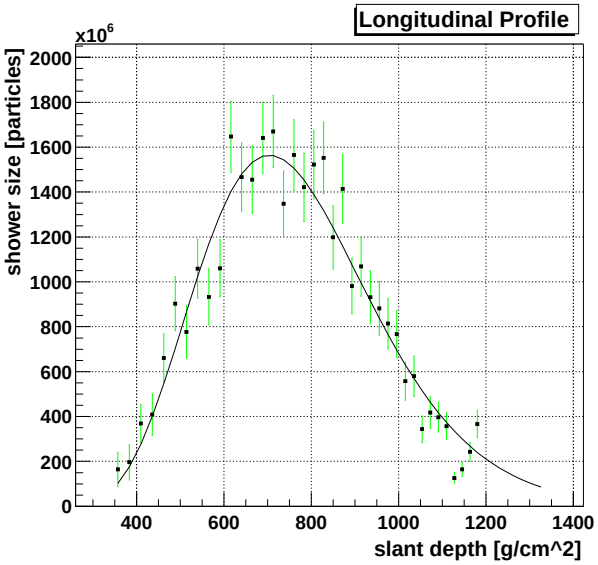

Figure 4. Reconstructed longitudinal profile of a shower landing about 16 km from the detector. The estimated energy is around 1.5×10^{18} eV. The line is a fit to a Gaisser-Hillas function.

5.6. Engineering Array results

During the Engineering Array (EA) run, a special trigger was set up to prove the ability of the system of detecting hybrid events that would fall under the 4-tank threshold required for normal operation. An online program was setup to reconstruct the shower geometry as seen by the FD in real time and therefore trigger the SD. 77 events where detected with this trigger.

To test the FD geometrical reconstruction capabilities, laser beams where fired at different positions and directions. The results from one of these tests is shown

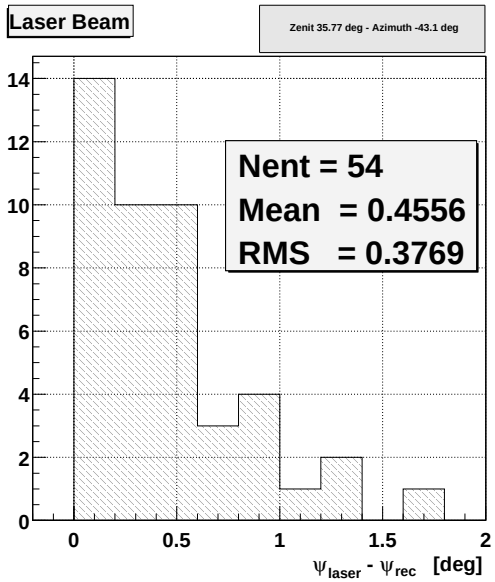

Figure 5. Angular difference between true and reconstructed geometry for a set of laser shot at the same direction.

in figure 5, where the true geometry is compared to the reconstructed geometry of the laser shot. These shots were performed aiming at a known star, therefore the direction is known with high precision. The laser position is measured using a GPS system. Studies are underway to determine the behavior of the error with shower inclination and impact parameter.
During the EA run, the detector was run for about 250 hours, corresponding to a duty cycle around 11%. Operations took place with up to 50% of moon illumination. The FD detected around 1000 shower candidates during the EA run. Analysis of these events is ongoing.

6. Conclusion

The Engineering Array phase demonstrated that the design requirements of Fluorescence and Surface detector are fulfilled and the implementation is satisfactory. The Auger Observatory is able to detect hybrid events and reconstruct them with the required precision. Further effort has started to complete the Observatory and answer the questions on UHECRs.

REFERENCES

1. M. Takeda et al. , Phys. Rev. Letters 81 (1998) 1163-1166
2. D.J. Bird, et al.1995, Ap.J., 441 144.
3. K. Greisen, Phys. Rev. Lett. 16 (1966) 748
4. G. Zatsepin and V. Kuzmin, JETP Lett. 4, 78 (1966)
5. D. Bergman, talk given at ICHEP 2002
6. Pierre Auger Observatory Technical Design Review, available `http://www.auger.org`
7. F. Kakimoto et al., Nucl.Instrum.Meth. A 372 (1996) 527-533
8. M. Ambrosio et al., Nucl. Instrum. Meth. A 478 (2002) 125-129
9. G. Borreani et al., IEEE Trans. Nucl. Sci. 48 3 (2001) 406
10. S. Argirò et al., IEEE Trans. Nucl. Sci. 48 3 (2001) 444